Journal of Renewable Energies

Revue des Energies Renouvelables

journal home page: https://revue.cder.dz/index.php/rer

Research paper

Enhancing wind power conversion efficiency with Vernier DSPM generator and sliding mode control

Abderrahmane Redouane [a,*] , **Rachid Saou** [a], **Cherif Guerroudj** [b,c], **Amrane Oukaour** [d]

[a] *Laboratoire de Génie Électrique, Faculté de Technologie, Université de Bejaia, 06000 Bejaia, Algeria.*

[b] *Laboratoire des systèmes électriques industriels (LSEI), BP N◦32 El Alia, Bab Ezzouar 1611, Alger, Algérie.*

[c] *Université de Lorraine - GREEN, 54000 Nancy, France.*

[d] *Laboratoire de Recherche en Sciences du Numérique GREYC, Université de Caen Normandie, 6 Boulevard du Maréchal Juin, 14032 Caen, France.*

ARTICLE INFO

Article history:
Received April 1, 2024
Accepted April 22, 2024

Keywords:
Direct driven
Low speed
DSPM
Wind turbine
Sliding mode control

ABSTRACT

To enhance the efficiency of wind power conversion systems, a DC conversion system that combines a wind turbine with a battery is introduced in this paper. The Vernier Doubly Salient Permanent Magnet (V-DSPM) generator at the center of this system, designed for low speeds and high torque, eliminates the need for troublesome gearboxes. The proposed control employs MPPT based on tip speed ratio with output as the reference current of the boost converter and a sliding mode control-based Gao's constant plus proportional rate reaching law to track the reference current. Three tests were performed to determine the efficiency of the proposed strategy. Moreover, a comparison with a conventional PI controller was carried out. The simulations were performed using MATLAB and Simulink. The obtained results show that the system with SMC has better performance than the system with PI.

1. INTRODUCTION

In recent years, wind power turbines have gained increasing popularity as an alternative to fossil fuels. Additionally, the growing demand for generators tailored to wind energy conversion, featuring higher power and torque densities has gradually increased (Kim et al., 2023). Conventional wind turbine generators are often equipped with gearboxes to achieve the required speed. However, these gearbox systems have many drawbacks, including being large, expensive, and require regular maintenance (Remli et al., 2023; Rezzoug et al., 2013). To overcome these problems, a special structure machine that operates at low speed, known as a slow machine or direct attack machine is proposed in (Saou et al.,

* *Corresponding author, E-mail address: abderrahmane.redouane@univ-bejaia.dz*

Tel : + 213 655781014

ISSN: 1112-2242 / EISSN: 2716-8247

2008). This innovative structure is called a Doubly Salient Permanent Magnet Machine (DSPM). Unlike traditional designs, its stator has a large number of teeth, and the rotor also has a large number of teeth and it does not contain windings or permanent magnets (PMs). The stator tooth step, τ_s, is identical to that of the rotor, τ_r. Instead, it is excited by non-rotating PMs, inset in the stator yoke (Saou et al., 2008). Nevertheless, the primary disadvantage of this machine is its tendency to produce a non-sinusoidal electromotive force (e.m.f.) and high electromagnetic torque ripples, leading to the generation of vibrations, and noise (Saou et al., 2008; Bekhouche et al., 2019). To mitigate the electromagnetic torque ripples and enhance the performance of the DSPM the paper (Guerroudj et al., 2017) proposes a Vernier Doubly Salient Permanent Magnet machine (V-DSPM). The Vernier effect in this new machine, as employed in the present study, is achieved by setting the stator tooth step, τ_s, to be different from that of the rotor, τ_r.

Furthermore, maximizing the output power of wind turbines presents a significant challenge in wind power control. Various methods have been presented in the literature. In (Yazıcı et al., 2019) a sensorless maximum power point tracking discrete-time integral terminal sliding mode controller (DITSMC) is developed to increase the energy efficiency of a WECS by reducing convergence-time and error-bounds. An integral sliding mode voltage regulator-based tip speed ratio (TSR) is proposed by (Yazıcı et al, 2017) to maximize turbine output power. The suggested method provides robust tracking capabilities. Paper (Dursun et al., 2020) presents a comparative study between tip speed ratio-based PI (TSR-PI) MPPT and perturbation & observation (P&O) MPPT. A Novel Hybrid MPPT is proposed by (Malobe et al., 2020). The suggested strategy uses a fuzzy controller to optimize the sliding mode controller. The main objective of the hybrid MPPT is to overcome certain problems of sliding mode control, such as the chattering phenomenon. A new maximum power point tracking controller based on voltage-mode Second-Order Fast Terminal Sliding Mode Control (SO-FTSMC) is proposed by (Dursun et al., 2020). The main purpose of the proposed control is to ensure that the system operates at the maximum power reference with enhanced effectiveness.

In this paper, a DC conversion system based on a wind power turbine and a battery is proposed. Our system utilizes a Vernier Doubly Salient Permanent Magnet generator, a non-conventional direct-drive machine. To extract the maximum power from the wind turbine, a proposed tip speed ratio based sliding mode control is employed to regulate the inner loop of the DC-DC boost converter. To assess the efficiency of the proposed control, three tests were conducted. The first test is performed with a constant load and constant wind speed, the second one involves varying the wind speed while maintaining a constant load, and the last one is carried out with variation in both parameters wind speed and load. Additionally, we provide a comparative analysis of our suggested technique with the conventional PI control method.

2. ENERGY CONVERSION SYSTEM CONFIGURATION

The system contains a wind turbine to capture wind power, a three-phase V-DSPM generator, a three-phase uncontrolled rectifier, a DC/DC boost converter to extract maximum power from the wind turbine, a battery with bidirectional DC/DC converter to regulate the DC bus and variable load. The global scheme is presented in Fig. (1).

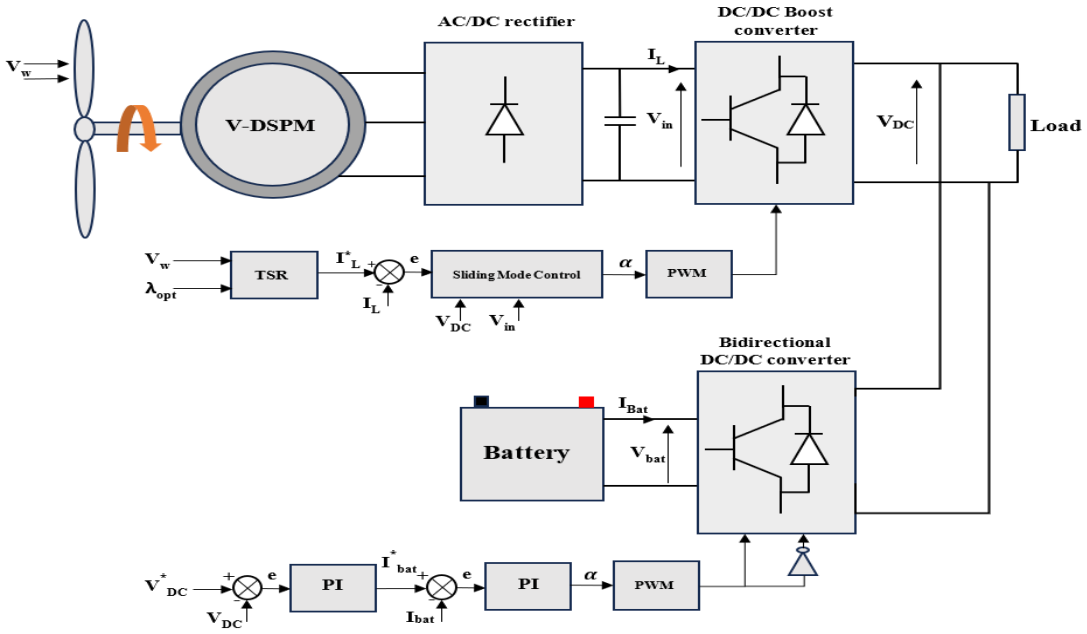

Fig 1. Proposed DC system

2.1 Wind turbine modeling

The following is an expression for aerodynamic power derived from wind kinetic energy:

$$P_t = 0.5\,\rho\,\pi\,R^2\,C_p(\lambda)\,V_w^3 \tag{1}$$

The power coefficient C_p depends on the tip speed ratio, tip speed ratio λ is given by:

$$\lambda = \frac{\Omega_t\,R}{V_w} \tag{2}$$

Where ρ, R, C_p, V_w, and Ω_t are, respectively, the air density, turbine radius, power coefficient, wind speed, and mechanical shaft speed.

2.2 V-DSPM modeling

The machine used in this study is a V-DSPM, a three-phase double-salient toothed-slot machine with a large number of rotor teeth and permanent magnets housed in the stator yoke (see Fig. (2)). The stator slots carry the windings of the three phases, while the rotor is passive, without any electrical windings.

In the stator of the V-DSPM machine, there are N_s = 48 teeth distributed across the 12 slots. We have maintained N_{ps}=12 slots and N_{dp}=4 teeth per slot. The number of teeth on the rotor, N_r = 64, is fixed to achieve a typical electrical frequency of 50 Hz at the nominal speed of 50 rpm (Guerroudj et al., 2017). The rotation speed of the DSPM is inversely proportional to the number of rotor teeth.

The V-DSPM is a conventional DSPM (Saou et al., 2008) that exploits the Vernier effect, achieved by having a rotor tooth pitch τ_r different from the stator tooth pitch τ_s.

$$\begin{cases} \tau_s = \dfrac{2\pi}{N_{seq}} \\ \tau_r = \dfrac{2\pi}{N_r} \end{cases} \tag{3}$$

N_{seq}, different from N_s, represents the number of stator teeth the machine would have if the stator armature were distributed-toothed and not slotted.

To ensure energy conversion and torque production, the studied structure must satisfy the following conditions (Guerroudj et al., 2017):

$$\begin{cases} \pm N_{seq} \pm N_r = \pm P \pm P_e \\ N_{seq} \neq 2P \neq 2P_e \\ N_r \neq 2P \neq 2P_e \end{cases} \quad (4)$$

P_e and P denote the number of magnet pairs and slot pairs per phase, respectively.

These conditions are met, for the machine, when considering N_{seq}=68 and N_{seq}=60. The machine with N_{seq}=68 demonstrates better performance according to (Guerroudj et al., 2017), which is why it was chosen for this study.

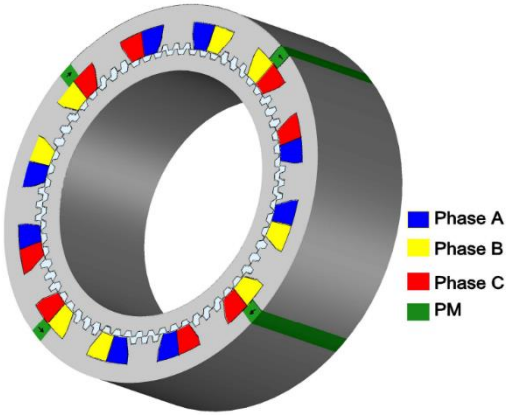

Fig 2. Cross-section of the studied Vernier Doubly Salient Permanent Magnet machine

The dynamic model of the V-DSPM is simplified using the Fourier transform. Terms of harmonics of order greater than 1 have been ignored. As a result, the V-DSPM's self-inductances, mutual inductances, and magnetic phase flux linkage concerning rotor position, obtained through the finite element method (FEM), can be respectively expressed as:

$$\begin{cases} L_a = L_0 + L_1 \cos\theta_e \\ L_b = L_0 + L_1 \cos\left(\theta_e - \frac{2}{3}\pi\right) \\ L_c = L_0 + L_1 \cos\left(\theta_e - \frac{4}{3}\pi\right) \end{cases} \quad (5)$$

$$\begin{cases} M_{ab} = M_{ba} = M_0 + M_1 \cos\left(\theta_e - \frac{4}{3}\pi\right) \\ M_{ac} = M_{ca} = M_0 + M_1 \cos\left(\theta_e - \frac{2}{3}\pi\right) \\ M_{bc} = M_{cb} = M_0 + M_1 \cos\theta_e \end{cases} \quad (6)$$

$$\begin{cases} \varphi_{ma} = \varphi_0 + \varphi_1 \cos\theta_e \\ \varphi_{mb} = \varphi_0 + \varphi_1 \cos\left(\theta_e - \frac{2}{3}\pi\right) \\ \varphi_{mc} = \varphi_0 + \varphi_1 \cos\left(\theta_e - \frac{4}{3}\pi\right) \end{cases} \quad (7)$$

Park transformation is applied for generator equations in the stator reference frame and the direct and quadrature voltage expressions of the V-DSPM in the d-q reference frame are given by:

$$\begin{cases} V_d = -\left(R_s + 2w_e M_{dq}\right)i_d + \frac{w_e}{2}\left(3L_d - L_q\right)i_q - L_d\frac{di_d}{dt} - M_{dq}\frac{di_q}{dt} \\ V_q = -\left(R_s - 2w_e M_{dq}\right)i_q - \frac{w_e}{2}\left(3L_q - L_d\right)i_d - L_q\frac{di_q}{dt} - M_{dq}\frac{di_d}{dt} - \sqrt{\frac{3}{2}}\varphi_1 w_e \end{cases} \quad (8)$$

R_s represents the stator resistance, i_d, and i_q denote the direct and quadrature currents, L_d and L_q signify the direct and quadrature inductances, M_{dq} stands for mutual inductance, we represent the electrical velocity and φ_1 represents the first harmonic of permanent magnet flux.

With:

$$\begin{cases} L_{dq} = L_0 - M_0 \pm \frac{1}{2}(L_1 + 2M_1)\cos 3\theta_e \\ M_{dq} = -\frac{1}{2}(L_1 + 2M_1)\sin 3\theta_e \\ \theta_e = \int w_e\, dt \end{cases} \quad (9)$$

θ_e represents the electrical position.

The direct and quadratic magnetic flux equations are:

$$\begin{cases} \varphi_d = L_d i_d + M_{dq} i_q + \sqrt{\frac{3}{2}}\varphi_1 \\ \varphi_q = L_q i_q + M_{dq} i_d \end{cases} \quad (10)$$

The electromagnetic torque T_{em} is written in Eq (11):

$$T_{em} = -\sqrt{\frac{3}{2}}N_r\varphi_1 i_q + \frac{1}{2}N_r\left(L_d - L_q\right)i_d i_q - \frac{1}{2}N_r M_{dq}\left(i_d^2 - i_q^2\right) \quad (11)$$

The mechanical equation is expressed as:

$$J\frac{d\Omega_t}{dt} = T_{em} - T_m - f\Omega_t \quad (12)$$

Active and reactive machine powers are expressed by the following equations:

$$\begin{cases} P = v_d i_d + v_q i_q \\ Q = v_d i_q - v_q i_d \end{cases} \quad (13)$$

On the other hand, Joule and iron losses are given by the following formulas:

$$\begin{cases} P_{cu} = R_s i_d^2 + R_s i_q^2 \\ P_{ir} = \frac{3}{2}N_r\Omega_t\left[M_{dq}\left(i_d^2 - i_q^2\right) - \left(L_d - L_q\right)i_d i_q\right] + \frac{1}{2}\left(L_d\frac{di_d^2}{dt} + L_q\frac{di_q^2}{dt}\right) + M_{dq}\frac{d(i_d i_q)}{dt} \end{cases} \quad (14)$$

The power factor can be evaluated with the help of the mean values of active and reactive powers as:

$$\cos\psi = \left|\frac{P_{mean}}{\sqrt{P_{mean}^2 + Q_{mean}^2}}\right| \quad (15)$$

3. CONTROLLER DESIGN

3.1 MPPT-based Tip speed ration

The MPPT strategy is used to determine the optimal operating point of the wind turbine. Several algorithms have been presented in the literature, such as Optimal Torque (OT) control, Tip Speed Ratio (TSR) control, Power Signal Feedback (PSF) control, and Perturbation and Observation (P&O) control.

In this paper, TSR control is chosen due to its several advantages, including simplicity of implementation, fast convergence speed, and high performance under varying wind speeds. Fig. (3) illustrates the TSR-based MPPT algorithm.

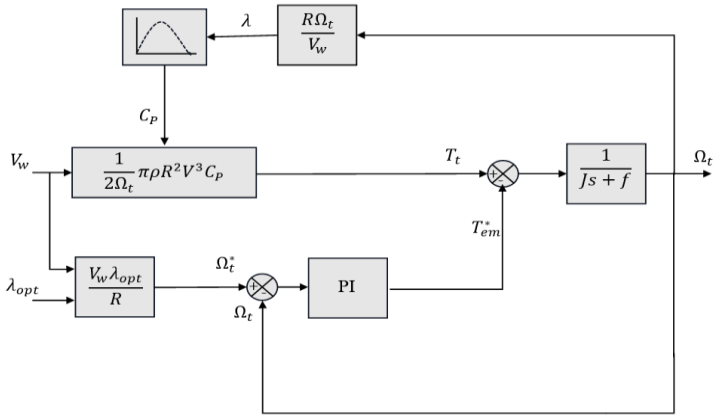

Fig 3. TSR-based MPPT algorithm

The wind turbine's C_p (λ) curve is presented in Fig. (4). The angle γ is set to zero due to the assumption of a fixed pitch rotor. It can be observed that the *Cp* has a single maximum point, C_{pmax} = 0.428 at λ_{opt} = 2.25.

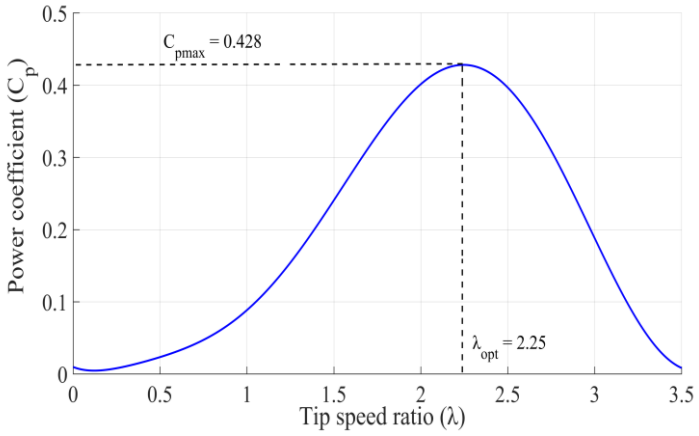

Fig 4. Wind turbine power coefficient C_p

3.2 Proposed sliding mode control current

Sliding mode control is a nonlinear control technique that can be applied to both linear and nonlinear systems. It is a robust control technique known for its excellent disturbance resistance and rapid dynamics response (Sami et al., 2020).

The first step involves defining the sliding surface. In this study, the sliding surface is defined as follows:

$$S = i_L^* - i_L \tag{16}$$

The sliding mode control signal is the sum of the equivalent and discontinuous control signals, and is given as follows:

$$u = u_{eq} + u_{dis} \tag{17}$$

The equation of the current inductor is given as follows:

$$\frac{di_L}{dt} = \frac{v_{in}}{L} - (1-u)\frac{v_{DC}}{L} \tag{18}$$

The Gao's low is given as follows (Bartoszewicz, 2015):

$$\dot{S} = -\alpha\, S - \beta\, sign(S) \tag{19}$$

From equations (16), (18), and (19), the sliding mode control signal-based Goa's law is obtained in Eq (20):

$$u = \frac{v_{DC} - v_{in}}{v_{DC}} + \frac{L(\alpha\, S + \beta\, sign(S))}{v_{DC}} \tag{20}$$

Where, $\alpha, \beta > 0$ are sliding mode parameters to be tuned.

The control signal block diagram is shown in Fig. (5).

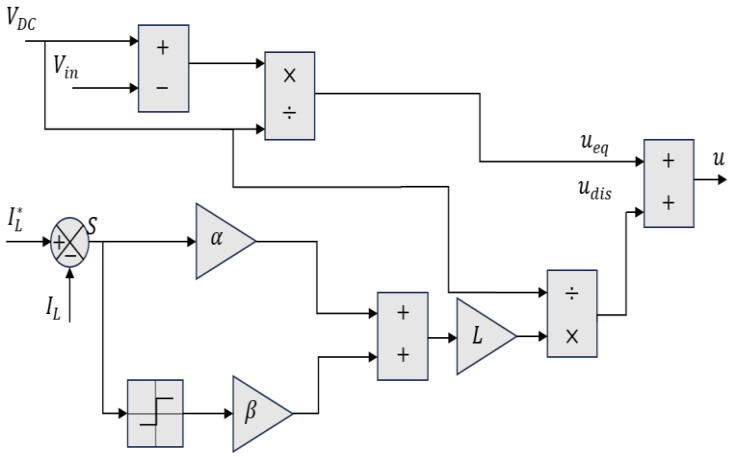

Fig 5. The proposed control method diagram

4. SIMULATION RESULTS

To verify the robustness of the proposed control method, three tests were carried out. Test (1) was performed with a constant load and constant wind speed, test (2) consisted of varying the wind speed while maintaining a constant load, and test (3) was carried out with variations in both wind speed and load.

Fig. (6), shows wind speed profile, with speed variations ranging from 5.5 m/s to 9.2 m/s. From 0 s to 5s the speed remains constant at 8m/s. From 5 s to 15 s, the speed varies. Fig. (7a) presents the V-DSPM speed, demonstrating that the generator speed follows the variation of the wind speed. Fig. (7b) shows the generator's high electromagnetic torque, which is a result of the low rotation speed of this generator. Fig. (8) displays the phase voltage and phase current of the V-DSPM. Fig. (9) presents the direct and the quadratic current of the V-DSPM generator.

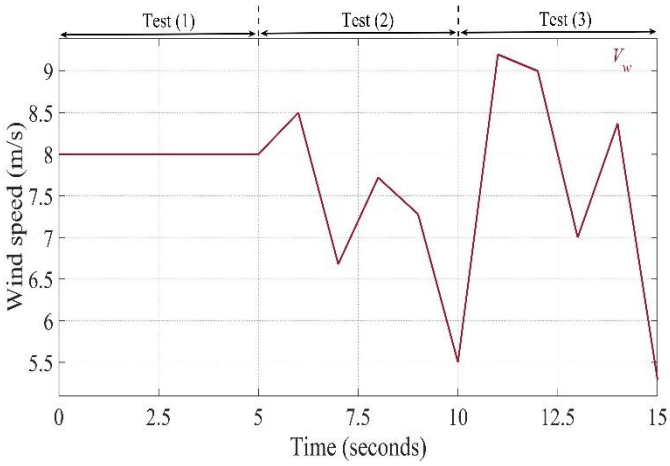

Fig 6. Wind speed profile V_w

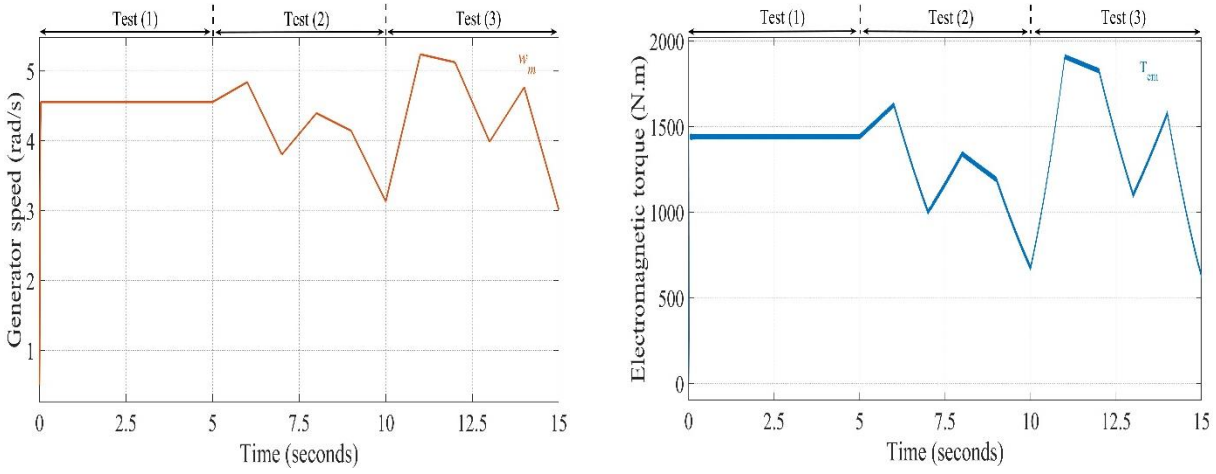

(a) (b)

Fig 7. Simulation results of (a) Generator speed Ω_m, (b) Electromagnetic torque generator T_{em}

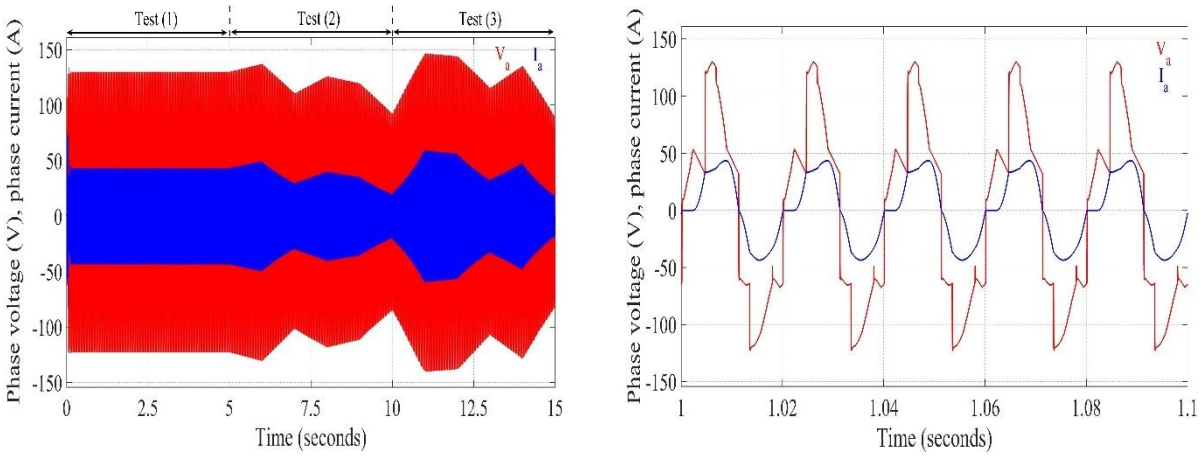

Fig. 8 Generator phase voltage and phase current V_a & I_a

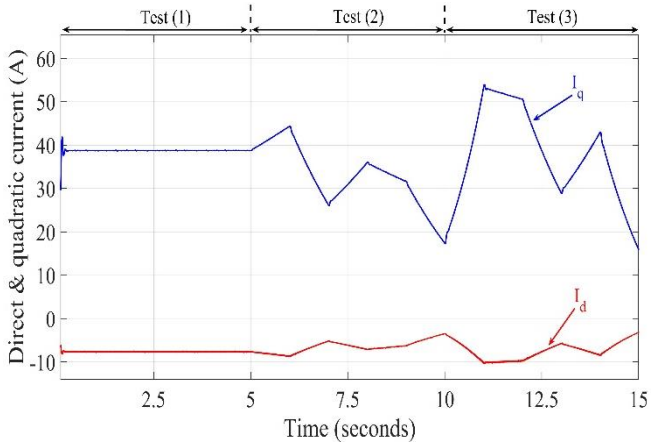

Fig. 9 V-DSPM direct I_d and quadratic I_q current

Figs. (10), (11), and (12) display the simulation results of DC/DC booster inductor current, wind turbine output power, and battery power under three different tests using the proposed control and conventional PI control. During the three tests, the proposed sliding mode control (SMC) converges to the maximum power point with a fast response compared to PI control. It can be observed that the SMC control exhibits higher efficiency in extracting the maximum power from wind turbines under varying wind conditions and load fluctuations. Table 1 summarizes the performance of the different techniques.

From Fig. (13), it is evident that the DC-bus voltage remains balanced even during disturbances and is maintained at the desired operating value of 500 V.

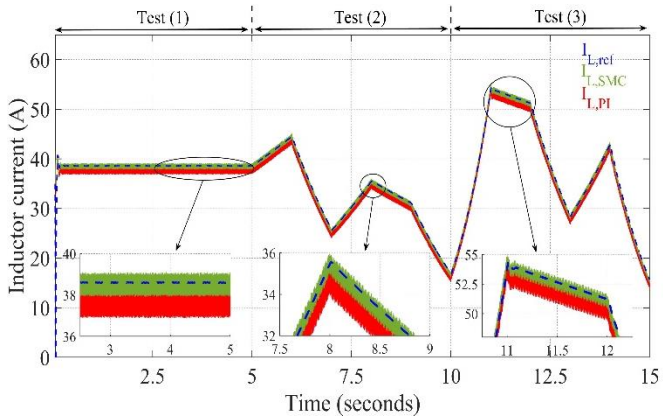

Fig. 10 Inductor current I_L

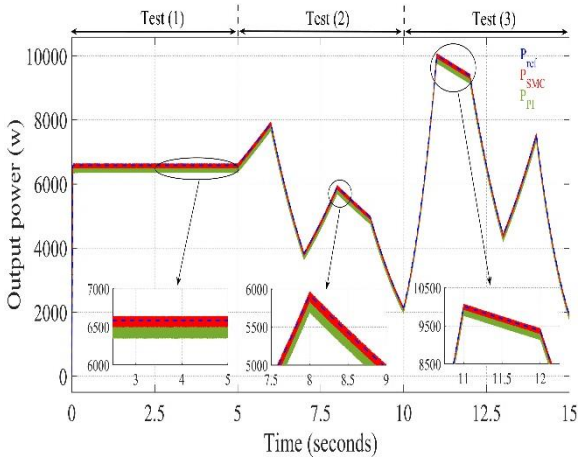

Fig. 11 Wind turbine output power P_{wind}

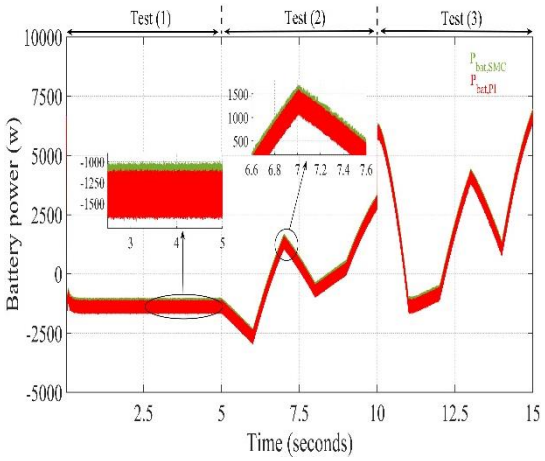

Fig. 12 Battery power P_{bat}

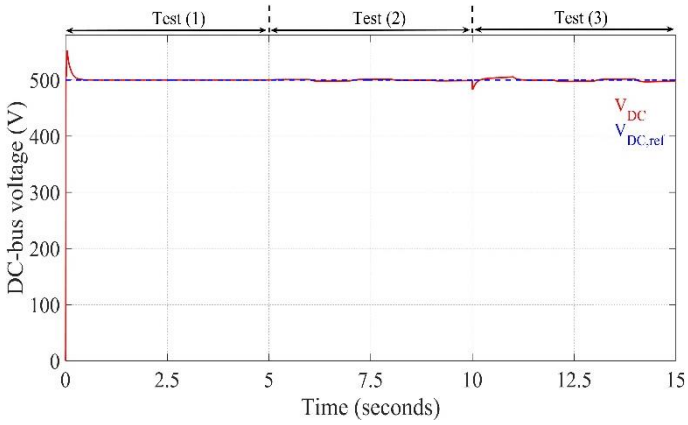

Fig. 13 DC-bus voltage V_{DC}

Table 1. Performance of the different techniques

	Test (1)		Test (2)		Test (3)	
Mean	PI	SMC	PI	SMC	PI	SMC
P_{wind} (w)	6486.4	6586.6	5395.8	5403.8	6675.1	6756.83
$I_{inductor}$ (A)	37.87	38.52	32.28	32.83	37.78	38.46

5. CONCLUSION

To enhance the efficiency of the wind power system, this paper proposes a non-conventional generator with low rotation speed and high electromagnetic torque. The purpose of using this type of generator is to eliminate the gearbox from the conversion system and address the associated issues such as large size, cost, power losses, and maintenance. Furthermore, a sliding mode control is suggested to optimize the output power of the wind turbine under different scenarios, including wind speed variations and load fluctuations. The simulation results demonstrate that the proposed control enhances the performance of the wind power system by maximizing power extraction.

APPENDIX

Table A1. V-DSPM parameters

Parameters
V_w: Wind speed (9.2 m/s)
C_{pmax}: maximum power coefficient (0.428)
λ_{opt}: Optimal tip speed ratio (2.25)
ρ: Air density (1.225 Kg/m^3)
R: Wind turbine radius (3.951 m)
P_n: Rated wind turbine power (10 kW)
Number of blades: 3

Table A2. Wind turbine parameters

Parameters
$R_{s:}$ Stator resistance (87.37 mΩ)
L_0: Continuous self-inductance (30.5 mH)
L_1: First harmonic self-inductance (1.4 mH)
M_0: Continuous mutual inductance (-15.5 mH)
M_1: First harmonic mutual inductance (6.7 mH)
φ_1: First harmonic permanent magnet flux (0.4147 Wb)
N_r: Number of teeth in the rotor (64)
N_s: Number of teeth in the stator (48)
N_{seq}: Number of equivalent teeth in the stator (68)
N_{ps}: Stator pole (12)
P: Number of magnet pairs (2)
P_e: Number of slot pairs per phase (4)
τ_r, τ_s: Rotor and stator tooth pitch
J: Rotor inertia (Nm s^{-1})
f: Viscous friction coefficient
P_n: Rated power (10 kW)
Ω_n: Rated rotor speed (50 rpm)

NOMENCLATURE

$Cos\ \psi$: Power factor
i_d, i_q: Direct and quadratic currents (A)
i_L: Inductance current of the DC/DC converter (A)
L_d, L_q: Direct and quadratic inductance (H)
M_{dq}: Mutual inductance (H)
P: Active power (W)
P_{cu}: Joule losses (W)
P_{ir}: Iron losses (W)
P_{mean}: Mean active power (W)
Q: Reactive power (VAR)
Q_{mean}: Mean reactive power (W)
S: Sliding surface
T_m: Mechanical torque (Nm)
T_{em}: Electromagnetic Torque (Nm)
u_{eq}, u_{dis}: Equivalent and discontinuous control signals
v_{in}: Input voltage (V)
v_{DC}: DC bus voltage (V)
v_d, v_q: Direct and quadratic voltages (V)
w_e: Electrical velocity (rad/s)

greek symbols
α, β: Sliding mode control parameters
φ_d, φ_q: Direct and quadratic flux (Wb)
θ_e: Electrical position (rad)

REFERENCES

Bartoszewicz A, (2015) A new reaching law for sliding mode control of continuous time systems with constraints. Transactions of the Institute of Measurement and Control. pp. 515-521. https://doi.org/10.1177/0142331214543298

Bekhouche L, Saou R, Guerroudj C, Kouzou A, Zaïm M E. (2019) Electromagnetic Torque Ripple Minimization of Slotted Doubly Salient-Permanent-Magnet Generator for Wind Turbine Applications. Progress In Electromagnetics Research M. pp.181-190. https://doi.org/10.2528/PIERM19052804

Dursun E H, Kulaksiz A A, (2020) Second-order Fast Terminal Sliding Mode Control for MPPT of PMSG-based Wind Energy Conversion System. Elektronika ir Elektrotechnika. https://doi.org/10.5755/j01.eie.26.4.25762

Dursun E H, Kulaksiz A A. (2020) MPPT Control of PMSG Based Small Scale Wind Energy Conversion System Connected to DC Bus. International Journal of Emerging Electric Power Systems. pp. 20190188. https://doi.org/10.1515/ijeeps-2019-0188

Guerroudj C, Saou R, Boulayoune A, Zaïm M E, Moreau L. (2017) Performance analysis of Vernier slotted doubly salient permanent magnet generator for wind power. International Journal of Hydrogen Energy. pp 8744-8755. https://doi.org/10.1016/j.ijhydene.2016.07.043

Kim H, Kang S, Jung S, et al. (2023) Design and Analysis of Permanent Magnet Vernier Machine for Direct-Driven Wind Power Generator Considering Pole-Slot Combinations. J. Electr. Eng. Technol. pp. 319–327. https://doi.org/10.1007/s42835-022-01231-y.

Malobe P, Djondine P, Eloundou P, Ndongo H. (2020) A Novel Hybrid MPPT for Wind Energy Conversion Systems Operating under Low Variations in Wind Speed. Energy and Power Engineering. pp. 716-728. https://doi.org/10.4236/epe.2020.1212042

Remli A, Guerroudj C, et al. (2023) Control of an Outer Rotor Doubly Salient Permanent Magnet Generator for Fixed Pitch kW Range Wind Turbine Using Overspeed Flux Weakening Operations. Actuators, pp. 168. https://doi.org/10.3390/act12040168.

Rezzoug A, Zaïm M E. (2013) Non-conventional electrical machines. John Wiley & Sons. https://doi.org/10.1002/9781118604373

Sami I, Ullah S, Basit A, Ullah N, Ro J S. (2020) Integral Super Twisting Sliding Mode Based Sensorless Predictive Torque Control of Induction Motor. In IEEE Access. pp. 186740-186755. https://doi.org/10.1109/ACCESS.2020.3028845

Saou R, Zaïm M E, Alitouche K. (2008) Optimal designs and comparison of the doubly salient permanent magnet machine and flux reversal machine in low-speed applications. Power Components Syst. pp. 914–931. https://doi.org/10.1080/15325000801960564

Yazici I, Yaylaci E K. (2017) Improving Efficiency of the Tip Speed RatioMPPT Method for Wind Energy Systems by Using an Integral Sliding Mode Voltage Regulator. J. Energy Resour. Technol. pp. 051203. https://doi.org/10.1115/1.4038485

Yazıcı I, Yaylacı E K. (2019) Discrete-time integral terminal sliding mode based maximum power point controller for the PMSG-based wind energy system. IET Power Electronics. pp. 3688-3696. https://doi.org/10.1049/iet-pel.2019.0106